Journal of Biomechanics 44 (2011) 2236–2242

Contents lists available at ScienceDirect

Journal of Biomechanics

journal homepage: www.elsevier.com/locate/jbiomech
www.JBiomech.com

Markerless analysis of front crawl swimming

Elena Ceseracciu [a], Zimi Sawacha [a], Silvia Fantozzi [b,c], Matteo Cortesi [b], Giorgio Gatta [b], Stefano Corazza [d], Claudio Cobelli [a,*]

[a] Department of Information Engineering, University of Padova, Via Gradenigo 6B, 35131 Padova, Italy
[b] Faculty of Exercise and Sport Sciences, University of Bologna, Italy
[c] Department of Electronics Computer Sciences and Systems, University of Bologna, Italy
[d] Mixamo Inc., U.S.A.

ARTICLE INFO

Article history:
Accepted 1 June 2011

Keywords:
Biomechanics
Video-based
Automatic
Underwater

ABSTRACT

Research on motion analysis of swimmers is commonly based on video recordings of the subject's motion, which are analyzed by manual digitization of feature points by an operator.

This procedure has two main drawbacks: it is time-consuming, and it is affected by low repeatability. Therefore, the application of video-based, automatic approaches to motion analysis was investigated. A video-based, markerless system for the analysis of arm movements during front crawl swimming was developed. The method proposed by Corazza et al. (2010) was modified in order to be used into water environment. Three dimensional coordinates of shoulder, elbow and wrist joints centers of 5 sprint swimmers performing front crawl swimming were determined. Wrist joint velocity was also calculated. Accuracy and reliability of the proposed technique were evaluated by means of comparison with traditional manual digitization (SIMI Reality Motion Systems GmbH). Root mean square distance (RMSD) values between trajectories estimated with the two techniques were determined. Results show good accuracy for wrist joint (RMSD < 56 mm), and reliability, evaluated on one subject, comparable to the inter-operator variability associated with the manual digitization procedure. The proposed technique is therefore very promising for quantitative, wide-scale studies on swimmers' motion.

1. Introduction

Analysis of swimmers' kinematics is a challenging problem in the field of sports biomechanics because of the difficult experimental conditions that affect the setup of motion capture devices.

The presence of water and the limited space available in swimming pools are some of the factors that hinder the use of electronic devices. For example, commercial stereophotogrammetric systems that employ reflective markers cannot be adopted. Hence, research on motion analysis of swimmers is commonly based on video recordings of the subject's motion. 2D analyses require a single camera; points of interest are digitized on each video and analysis of movement on the sagittal plane is performed (Holthe and McLean, 2001). Since the motion in front-crawl swimming occurs on different planes (Schleihauf et al., 1983), for a descriptive analysis of three-dimensional (3D) motion a multi-camera setup is needed, which requires not only calibration, but also synchronization of the cameras. These procedures are hindered by the underwater experimental environment (Gourgoulis et al., 2008): refraction of light rays causes image deformations, yielding to lower accuracy, and the equipment must comply with safety regulations. Furthermore, videos are analyzed by manual digitization of feature points on all images, which may correspond to either visual markers drawn on the subject or crucial points, such as joint centers, identified by the operator. This procedure has two main drawbacks: it is time-consuming and can easily lead to misidentification of features, especially when a large number of points are involved. Recently, the adoption of markers constituted of Light Emitting Diodes has been introduced (Slawson et al., 2010). These allow to automate the tracking process, but investigation so far has only regarded identification of areas instead of single points, and motion on the sagittal plane. Alternative approaches based on accelerometric sensing units have also been adopted (Ohgi, 2002; Slawson et al., 2008; Callaway et al., 2009). This technology is relatively cheap and provides higher sampling rates; however, processing and interpretation of measured data is not straight-forward. Furthermore, sensing units may encumber the subject, which hinders their application for analysis of swimmers' performances during competitions.

In this context, the application of video-based, markerless approaches to motion analysis were investigated (Sigal and Black,

* Corresponding author: Tel.: +39 049 8277803.
E-mail address: cobelli@dei.unipd.it (C. Cobelli).

0021-9290/$ - see front matter © 2011 Elsevier Ltd. All rights reserved.
doi:10.1016/j.jbiomech.2011.06.003

2010). These approaches do not require to draw or attach markers to the athlete skin, thus are suitable for sport quantitative analysis during training or even competition. To the authors' knowledge however, no quantitative markerless analysis of swimming has been performed to date. A semi-automatic method to synthesize underwater motion by adjusting a "virtual human" model to the morphology of the subject has been proposed (Aguiló et al., 2004), but no biomechanical validation has been carried out. The approach proposed in Corazza et al. (2006) and Mündermann et al. (2006), that relies on video sequences of the subjects to automatically estimate their kinematics, was taken as starting point for the development of a novel underwater markerless motion capture system. This approach indeed has been successfully adopted in the clinical field (Corazza et al., 2007) and to evaluate healthy subjects while performing a 30° sidestep cutting task on different surfaces at a constant speed (Dowling et al., 2010).

The aim of our study is to investigate the applicability of markerless motion capture to kinematics analysis of front crawl swimming. The motion of one arm has been investigated so far, as it is the key feature in characterizing the crawl. The accuracy of the proposed technique has been evaluated with respect to a commercial video-based motion analysis system that requires manual digitization of points. Inter- and intra-operator repeatability of the digitization process have been evaluated, as a measure of the precision of the gold standard technique.

2. Materials and methods

2.1. Data acquisition

Five sprint swimmers (mean age 22.8 ± 2.2 years, mean height 1.80 ± 0.04 m, mean weight 79.2 ± 11.3 kg) participated in this study, and performed a front-crawl swimming trial at self-selected speed while being filmed with six underwater color analog wide-angle cameras with 720×576 pixel resolution (TS-6021PSC). Cameras were positioned following indications from literature (Mündermann et al., 2005), as far as the swimming pool environment permitted. The position of all cameras is shown in Fig. 1. Each camera was connected to a FireWire (IEEE 1394a)-equipped notebook through an Analog to Digital Video Converter (Canopus ADVC55; output DV video, PAL interlaced, 25 frames/s). The system was synchronized automatically employing a custom-made software application, which routes through a local area network the start and stop signals. The synchronization delay was found to be inferior to a frame duration, which in our study is 20 ms. A total of 4 notebooks was used; out of them, 2 were equipped with PCMCIA IEEE 1394a cards and could therefore be connected to two cameras. Calibration of the intrinsic parameters of each camera was performed in dry conditions, filming a black and white checkerboard, as indicated in the Calibration Toolbox for Matlab by J.Y. Bouguet (http://www.vision.caltech.edu/bouguetj/calib_doc/), which was used for parameters estimation. Intrinsic parameters were then corrected for underwater application (Lavest et al., 2003). Focal length was multiplied by 1.333, while 2nd order and 4th order radial distortion parameters were divided, respectively, by 1.333 and $1.333\dot{3}$. After camera placement in the swimming pool, extrinsic calibration was performed by means of a 12-control points calibration grid ($2\text{ m} \times 1.1\text{ m} \times 1.1\text{ m}$). This two-step calibration procedure allows to minimize the operations to be accomplished underwater while maintaining a more accurate camera distortion model than common DLT-based algorithms (Heikkila and Silven, 1997).

2.2. Video processing and silhouette extraction

An overview of the markerless processing pipeline is provided in Fig. 2. In a pre-processing phase, videos were uncompressed and bob deinterlaced using the "Smart Bob Filter for VirtualDub" by Donald Graft. The resulting videos are subjected to a silhouette extraction process, in which the areas of the image that represent the swimmer are detected.

Underwater recordings are characterized by a variable, unstill background; this is caused by the movement that occurs in water when the swimmer passes through. Therefore simple background subtraction approaches based on intensity and color threshold (Mündermann et al., 2007), that are used in controlled environments such as gait analysis laboratories, cannot be employed. An adaptive background subtraction technique was adopted instead: a model of the distribution of color values for each pixel of an image was created, then updated iteratively over each frame of the video sequence. The Gaussian Mixture model (GMM) has been employed for its versatility and easy mathematical formulation (KadewTraKuPong and Bowden, 2001). For each frame, the current RGB value of each pixel is checked against the correspondent GMM; it is classified as belonging to the background if it is well described by the greater components of the model. Additional silhouette extraction errors are caused by the presence of foam generated by the movements of the subject. In order to reduce this type of artefacts, an additional component was created for the background model of all pixels; its mean value corresponds to a typical *foam* RGB value measured from a video. For cameras placed on the bottom of the swimming pool and facing upwards, an additional hard-thresholding step was also performed: pixels for which the sum of red, green and blue color values exceeds an heuristically determined value are considered as background. This allows to achieve greater shape definition, exploiting the fact that the area occupied by the subject is darker than the surroundings, since external light is blocked (Fig. 3).

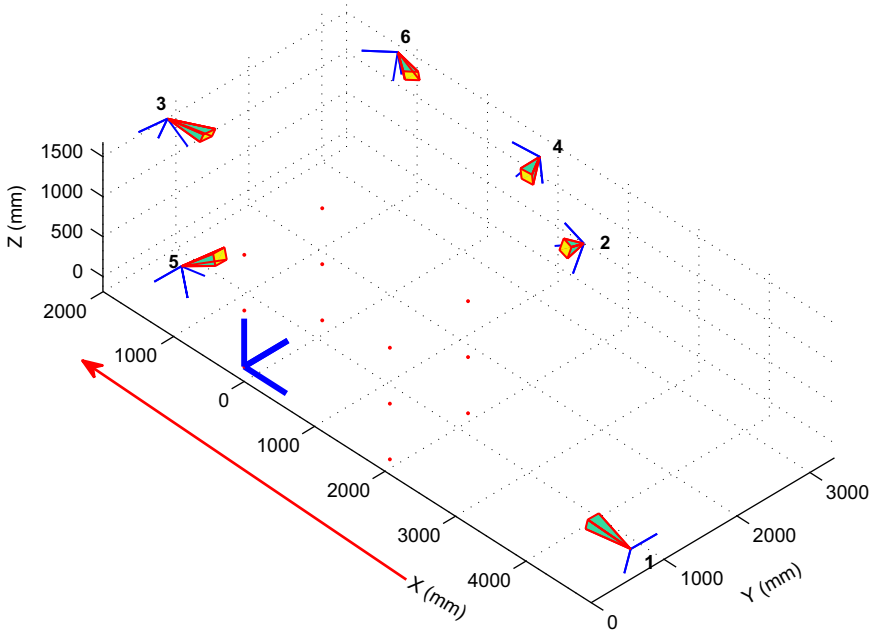

Fig. 1. Camera setup for the experiments in this study; coordinates are expressed in centimeters, the origin of the frame of reference is indicated by the blue lines, the red points correspond to the control points on the grid. Direction of swimming is indicated by the red arrow. (For interpretation of the references to color in this figure legend, the reader is referred to the web version of this article.)

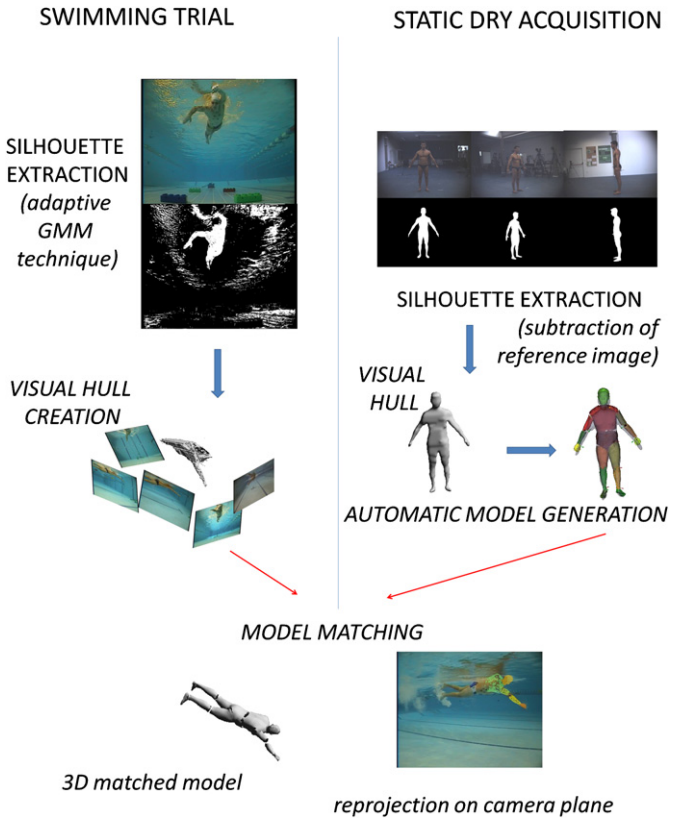

Fig. 2. Overview of the markerless processing pipeline that thas been followed.

2.3. Visual hull creation

A visual hull represents the maximum volume occupied by a 3D entity that explains all its projected silhouettes. It is therefore a locally convex over-approximation of the volume occupied by the subject at each instant (Corazza et al., 2006; Laurentini, 1994). For this study, visual hulls were reconstructed with 0.01 m voxel resolution.

2.4. Model

In order to obtain kinematic information from the visual hull, it is necessary to identify the clusters of mesh vertices that belong to each body segment. A segmented, articulated model was therefore fit into visual hull data. This full-body model was automatically generated from a static, dry visual hull of the subject in a reference pose (Corazza and Gambaretto et al., 2010) (Fig. 4). It consists of:

- a triangular mesh, which represents the shape of the subject. Each vertex in the mesh is labeled as belonging to a body part. Fifteen body parts are considered (head, torso, pelvis, arms, forearms, hand**s**, shanks, thighs, feet);
- a set of joint centers, expressed as 3D points in the mesh frame of reference. Each joint connects two body parts;
- a kinematic chain, which links body parts in a hierarchical way: all segments, except the root, have a "parent" segment.

The definition of the kinematic chain was modified to adapt to the focus of this study, that is the analysis of right arm motion: the chain starts at the right hand (root segment), then continues with right forearm, upper arm and torso; the latter has the head, the left arm, and the pelvis as children. Torso, pelvis and the inferior part of the body were instead considered as a rigid body. The following joint centers were therefore taken into consideration:

- wrist, connecting hand (parent segment) and forearm (child segment);
- elbow, connecting forearm (parent segment) and upper arm (child segment);
- shoulder, connecting upper arm (parent segment) and torso (child segment).

2.5. Model matching

The pose of each model segment was expressed in terms of roto-translation (6 degrees of freedom) of their embedded frame of reference with respect to the

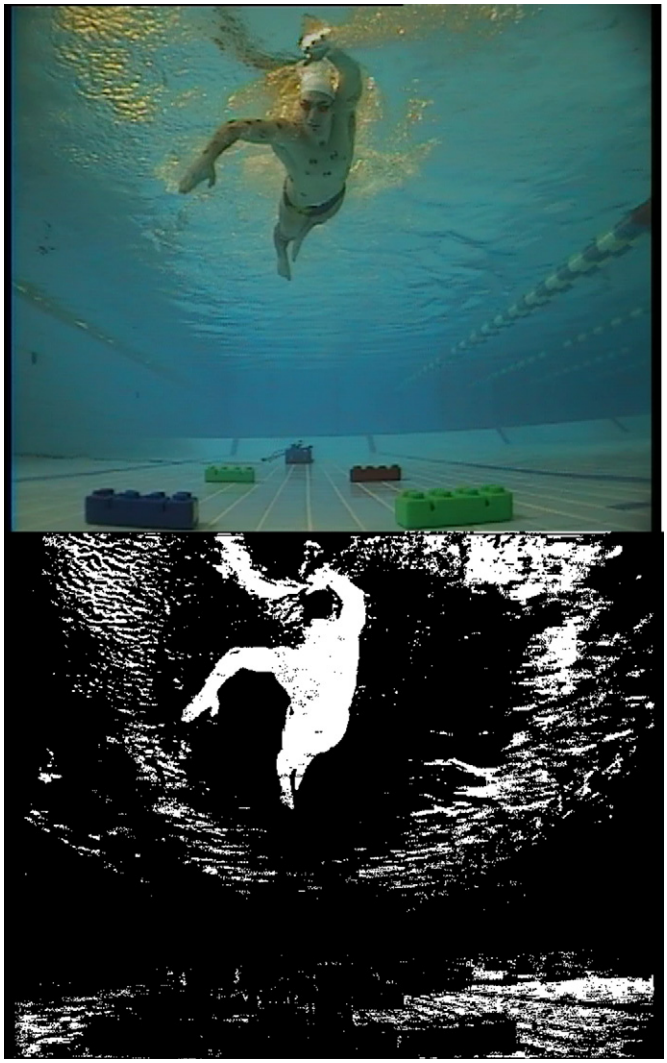

Fig. 3. Frame of a video sequence (above) and the result of the foreground extraction process (below: foreground in white, background in black).

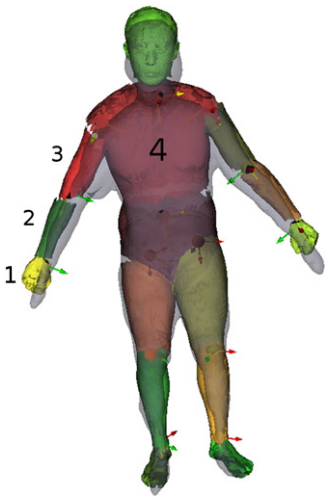

Fig. 4. Segmented model of the subject, obtained from a static, dry visual hull. Numbers indicate the sequence of the kinematic chain. The hand is the root segment; torso, pelvis and the inferior part of the body are considered as a rigid body.

parent segment. Therefore the parameters that describe the kinematics of the model were considered equal to the number of body parts under investigation, multiplied by six; the root segment parameters in fact represent its pose with respect to the global frame of reference. It should be noticed that the aim of the model matching process is to find the optimal pose of the model (i.e., identify the parameters) that explains the shape of the subject as reconstructed in the visual hull. Optimality can be defined as least-square minimization of the distance between vertices on the model mesh and corresponding vertices on the visual hull. The correspondence however is not known; indeed it has to be established by the matching process itself. Furthermore, the position of a vertex on the model mesh is a non-linear function of the roto-translation parameters of the body segment that it belongs to, and all body segments that connect it to the root segment. Therefore, global minimization of a non-linear cost function for all possible combinations of corresponding points on the two meshes is infeasible. The articulated-Iterative Closest Point (ICP) algorithm proposed in Corazza et al. (2010) was adopted herein; it is based on the ICP registration algorithm (Besl and McKay, 1992), and iterates between the following steps:

1. find the matching pairs between the vertices in the two meshes;
2. find the optimal model parameters that minimize the squared distance between paired vertices.

In this experiment, step 1 was performed identifying, for each vertex VH_i on the visual hull, the corresponding closest vertex M_i on the whole-body model (minimum Euclidean distance). This allows to deal with missing-data situations (i.e. part of the subject is not in view from all cameras), but makes the algorithm less robust to "phantom volumes" in the visual hull, caused by concavities or self-occlusion. In step 2 instead, only the paired vertices in which M_i belong to upper body segments are considered for the construction of the minimization problem. Additional details concerning the model matching algorithm can be found in Corazza et al. (2010).

Once segments' pose has been estimated, coordinates of joint centers in the global frame of reference are determined as the origin of the frame of reference embedded in the "child" segment related to each joint.

2.6. Evaluation of the technique's reliability

In order to test the accuracy of the here proposed methodology, joint trajectories obtained automatically with the markerless technique were compared with trajectories reconstructed, through traditional manual digitization, by means of the commercial software SIMI Motion (SIMI Reality Motion Systems GmbH). For one subject, five operators were required to manually digitize coordinates of shoulder, elbow, and wrist joints on each frame of the video sequences from all cameras, and results were compared (inter-operator variability). All the five operators were familiar with manual digitization. Joint positions were digitized only if the joint was completely underwater. Markers had been drawn on the subjects, but the operators were asked not to consider them for the identification of joint centers. In addition, one of the operators performed the manual digitization five times, as to assess intra-operator variability. Mean and standard deviation (SD) curves were calculated for each coordinate of each joint's trajectory, in both conditions. Root mean square distance (RMSD) was calculated to quantify the agreement between mean curves reconstructed with the manual digitization and coordinate curves reconstructed with the markerless technique. Distance between the reconstructed trajectories was compared to the SD that characterizes the variability of the manual tracking technique. Velocity of wrist joint has also been calculated by differentiation of low-pass filtered (zero-lag 3rd-order Butterworth filter, cutoff frequency: 3 Hz) wrist trajectories. RMSD between markerless trajectories and a single manual digitization by one operator have finally been calculated.

3. Results

Each front-crawl trial was processed by a computer in 2–3 h with the markerless method, while each repetition of the traditional procedure required 6–7 h of digitizing by an operator. Fig. 5 shows the trajectories obtained, for the first subject, with the markerless (red dotted line) and manual tracking technique by multiple operators (solid lines). The following phases have been identified from the videos by an expert, according to Maglischo (2003), for the underwater phase of the stroke: (A) gliding, (B) downsweep, (C) insweep, (D) upsweep, and (E) exit. A good agreement is demonstrated especially for wrist joint in all directions. For elbow and shoulder joints, greatest errors were found along the longitudinal direction. The markerless approach was not able to reconstruct joint trajectories during C and D phases.

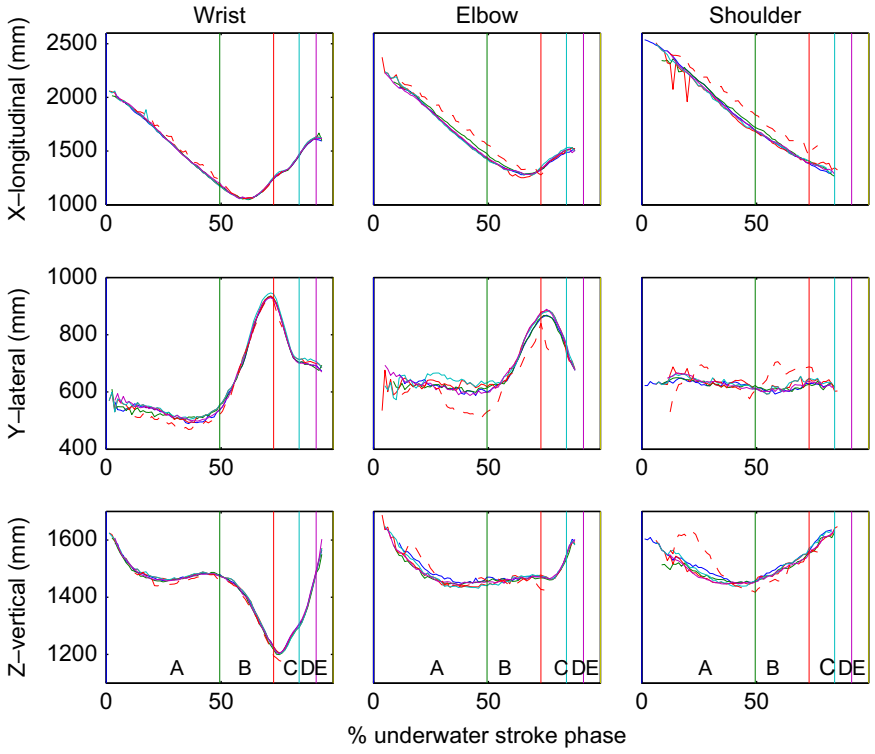

Fig. 5. Trajectories reconstructed through digitization by 5 operators employing a commercial software (solid lines) and with the markerless technique (red dotted line). The following phases are identified for the underwater phase of the stroke: (A) gliding, (B) downsweep (C) insweep (D) upsweep and (E) exit. (For interpretation of the references to color in this figure legend, the reader is referred to the web version of this article.)

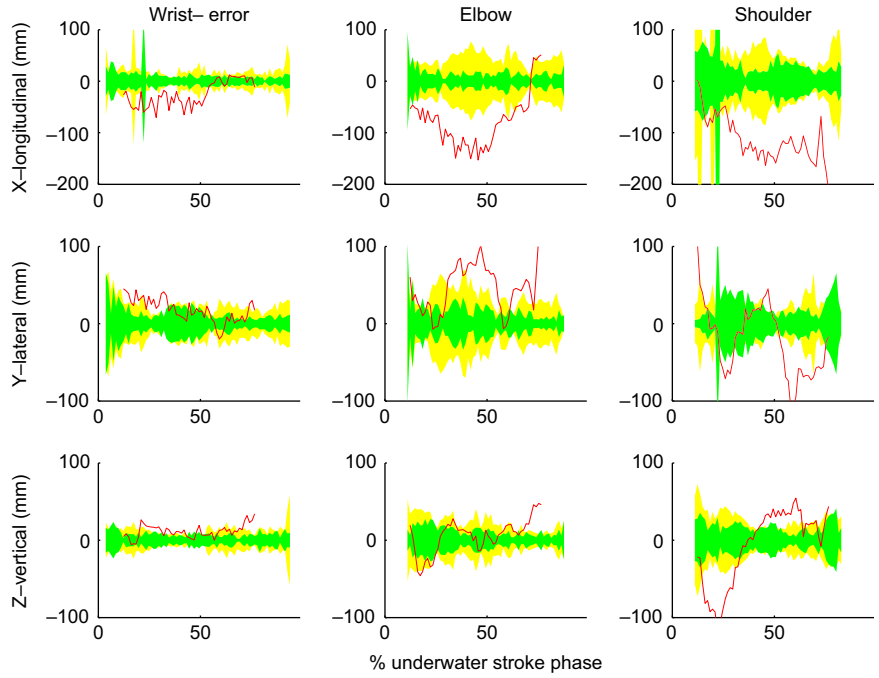

Fig. 6. Difference between trajectory coordinates estimated with markerless and averaged manual-tracking techniques (red line). ±3 standard deviation curves calculated on manual-tracking trajectories are shown in yellow (digitization by five operators) and green (five repetitions by one operator). (For interpretation of the references to color in this figure legend, the reader is referred to the web version of this article.)

Table 1
RMSD values between markerless and average manual-tracking trajectories (left column); maximum SD values for manual-tracking reconstructed curves are reported in middle (inter-operator) and right (intra-operator) columns.

	RMSD (mm)	Max. SD (inter operator)	Max. SD (intra operator)
Shoulder			
X	120.7	129.6	203.1
Y	50.4	21.8	40.5
Z	48.6	24.2	17.5
Elbow			
X	92.8	25.37	41.4
Y	56.5	23.3	30.3
Z	22.3	17.7	8.6
Wrist			
X	34.9	40.9	40.0
Y	23.0	22.6	21.9
Z	14.4	19.4	7.9

Fig. 6 shows the distances between the markerless and average manual-tracking trajectories (red line), compared to ±3 SD curves (yellow: digitization by five operators, green: five repetitions by one operator). The longitudinal direction proves to be the most critical one for all joints. RMSD values between markerless and average manual-tracking trajectories are reported in Table 1, for each coordinate, along with maximum SD values for manual-tracking reconstructed curves. While taking into account the wrist joint, the reported distance (14.4–34.9 mm) is comparable to the precision that can be achieved employing the commercial software (maximum SD: 40.9 mm). When considering both elbow and shoulder joints, it can be noticed that there is a relevant systematic error along the longitudinal (*X*) direction (see Table 1). Wrist joint velocity, calculated from low-pass filtered trajectories, is shown in Fig. 7; RMSD values are, respectively, 0.17, 0.08 and 0.14 m/s for *X*, *Y* and *Z* direction. Table 2 shows average RMSD between markerless and manual digitization techniques over the five subjects, and the relative SD. Best reconstruction accuracy is confirmed for wrist joint, while longitudinal direction proves to be the most critical.

4. Discussion

Upper arm 3D kinematics during front crawl stroke was reconstructed by means of an automatic markerless technique that was tailored to operate properly underwater. Even though it has been suggested that the arm trajectory during swimming is mainly described in a mediolateral plane, the mass of the literature reported only 2D dimensional analysis of swimming, and specifically on the sagittal plane (Holthe and McLean, 2001; Chollet et al., 2000). It should be further considered that quantitative data on stroke pattern characteristics are important in order to evaluate whether the differences between swimmers are mainly due to differences in stroke at specific paces, or differences between paces, or difference in physiological characteristics (Deschodt et al., 1996; Chollet et al., 2000). However, in this contest, results are contradictories due to a lack of data supporting one theory or the other.

The 3D markerless kinematic analysis was performed employing common out-of-shelf subacqueous cameras. Main modifications with respect to the literature regard the calibration procedure and the advanced image analysis algorithms that were employed. The kinematic properties of the model were specialized for the analysis of arm kinematics. The hand was chosen as root segment of the kinematic chain instead of the trunk in order to allow joint trajectory reconstruction in the initial phase of the stroke, when only the arm is in view of all cameras. For a couple of subjects however, the presence of foam around the hand at the beginning of *downsweep* phase (phase B in Figs. 5 and 7) caused a clearly incorrect pose estimation for the whole arm, which resulted in increased reconstruction errors. Joint trajectories estimation accuracy was evaluated in terms of RMSD with respect to trajectories obtained with a conventional 3D reconstruction technique, implemented in commercially available software.

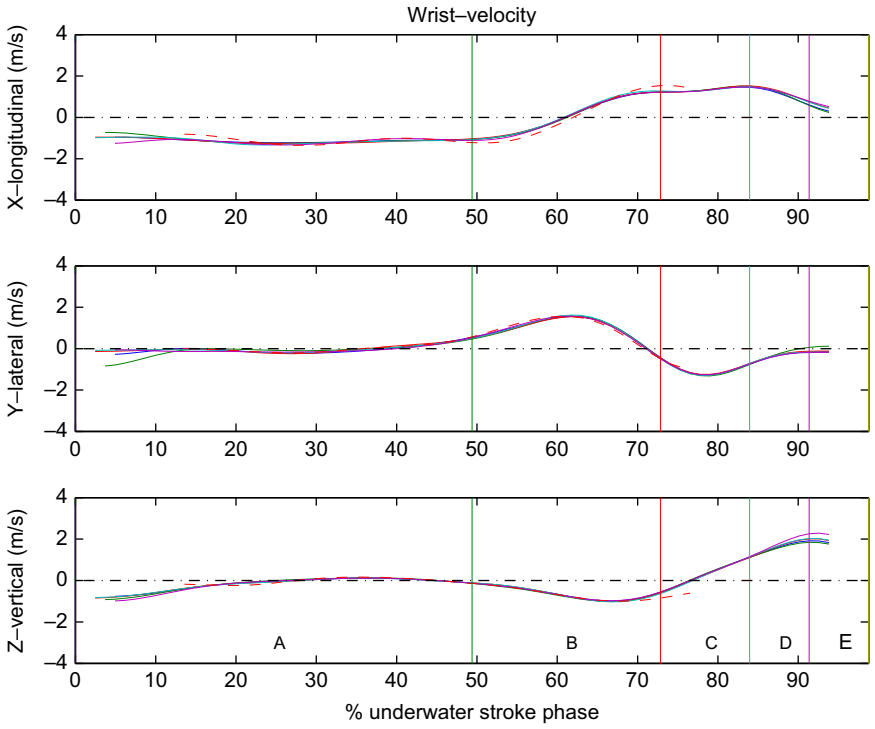

Fig. 7. Velocity of wrist joint center calculated from trajectories reconstructed through digitization by five operators employing a commercial software (solid lines) and with the markerless technique (red dotted line). (For interpretation of the references to color in this figure legend, the reader is referred to the web version of this article.)

Table 2
RMSD values between markerless and manual-tracking trajectories: average (left column) and standard deviation (right column) over the five subjects.

	Mean RMSD (mm)	Standard deviation of RMSD (mm)
Shoulder		
X	135.3	56.2
Y	76.2	36.7
Z	84.4	48.1
Elbow		
X	102.3	16.1
Y	83.7	17.4
Z	47.4	21.4
Wrist		
X	55.7	20.4
Y	26.8	11.1
Z	41.5	15.3

Accuracy at wrist joint level is deemed to be sufficient; this is most important for the technical analysis of the stroke, as hand trajectory is commonly used to identify and characterize stroke phases (Maglischo, 2003). For example, the stroke of the first subject of this study presents a *downsweep* phase (phase B in Figs. 5 and 7) characterized by a downward displacement of 26 cm and a contemporary outward movement of 40 cm. In this same phase, the reaching of *catch* position can be identified as occurring at 60% of the underwater stroke period by the sign change in velocity along the *X*-axis. Similarly, beginning of *insweep* phase is clearly indicated by sign change of velocity along the *Y*-axis (73% of underwater stroke period). Larger errors occur instead for elbow and shoulder joints. Systematic difference in the sagittal plane can be due to different joint models between the two techniques, and the rigid-body assumption that is introduced in the definition of the kinematic model for markerless analysis. In this context, the significant surface deformations that occur on the body during the execution of the movement are not taken into consideration, instead higher translational freedom is allowed between body segments. Higher translations however can lead to artefacts in the identification of the joint centers. This is particularly exacerbated, at shoulder level, by the presence of "phantom volumes" in the visual hulls reconstructed for some part of the stroke. This phenomenon occurs because the limited number of views causes spurious volumes to be recognized as occupied by the subject, indeed they are explained by the available silhouettes. The swimming pool environment, which limits possible camera placement positions, aggravates this drawback; for example, placing cameras on the bottom of the pool reduces excessively the reconstruction volume, and cameras cannot be positioned too close to the water–air interface, because the waves caused by the swimmer's movement would affect the quality of the images in a significant way.

Further limitations of the proposed method lie in the requirement that the whole body under investigation must be in view at all times, therefore reconstruction for the initial and final phases of the stroke, when the arm is partially out of water, is not currently possible. Information from out-of-water cameras cannot be easily integrated with the underwater views because of the issues related to the water–air interface, i.e. waves and foam.

The results obtained with the markerless technique are however encouraging, as this method allows 3D kinematics estimation in an automatic way, reducing processing time and costs. Wide-scale studies are therefore made possible, which can investigate differences in stroke patterns among a group of subjects, or identify performance indices for athletes' evaluation. In addition, the relaxation on the marker drawing requirement allows this technique to be adopted not only in controlled conditions, but also during competitions. This method could also be easily applicable to the other asymmetric swimming stroke (i.e., backstroke), while for symmetric swimming strokes, breaststroke and butterfly, self-occlusion would influence the reconstruction of the visual hull. Since the swimmer's volume is reconstructed, more complete analyses are possible, also in terms

of drag quantification. Upon reconstruction of both arms' motion, symmetry evaluation could finally be performed.

Further studies should concentrate on the investigation of a deformable arm model, following for example the method proposed in Cagniart et al. (2010); a hybrid approach, in which a small set of skin features are tracked and employed for pose estimation, could also provide more robust and accurate estimation of all three joint trajectories and trunk position.

Conflict of interest statement

Each of the authors does not have any conflict of interest.

Acknowledgements

The authors thank the contribution of Andrea Galletti, Andrea Giovanardi, Silvia Del Din, Stefano Ceccon and Giulia Donà for their help in collecting the data.

References

Aguiló, A., Martinez, P., Buades, J.M., Perales, F.J., González, M., 2004. Human motion analysis and synthesis using graphical biomechanics models applied to disable swimming people. In: Proceedings of the 3rd International Workshop on Virtual Rehabilitation, Lausanne, Switzerland.

Besl, P.J., McKay, N.D., 1992. A method for registration of 3-D shapes. IEEE Transactions on Pattern Analysis and Machine Intelligence 14 (2), 239–256.

Cagniart, C., Boyer, E., Ilic, S., 2010. Probabilistic deformable surface tracking from multiple videos. In: Proceedings of the 11th European Conference on Computer Vision (ECCV 2010), Crete, Greece.

Callaway, A., Cobb, J.E., Jones, I., 2009. A comparison of video and accelerometer based approaches applied to performance monitoring in swimming. International Journal of Sports Science and Coaching 4 (1), 139–153.

Chollet, D., Chalies, S., Chatard, J.C., 2000. A new index of coordination for the crawl: description and usefulness. International Journal of Sports Medicine 21 (1), 54–59.

Corazza, S., Gambaretto, E., Mündermann, L., Andriacchi, T.P., 2010. Automatic generation of a subject-specific model for accurate markerless motion capture and biomechanical applications. IEEE Transactions on Biomedical Engineering 57 (4), 806–812.

Corazza, S., Mündermann, L., Andriacchi, T., 2007. A framework for the functional identification of joint centers using markerless motion capture, validation for the hip joint. Journal of Biomechanics 40 (15), 3510–3515.

Corazza, S., Mündermann, L., Chaudhari, A.M., Demattio, T., Cobelli, C., Andriacchi, T.P., 2006. A markerless motion capture system to study musculoskeletal biomechanics: visual hull and simulated annealing approach. Annals of Biomedical Engineering 34 (6), 1019–1029.

Corazza, S., Mündermann, L., Gambaretto, E., Ferrigno, G., Andriacchi, T.P., 2010. Markerless motion capture through visual hull, articulated ICP and subject specific model generation. International Journal of Computer Vision 87 (1–2), 156–169.

Deschodt, V.J., Rouard, A.H., Monteil, K.M., 1996. Relationships between the three coordinates of the upper limb joints with swimming velocity. In: Troup, J.P., Hollander, A.P., Strasse, D., Trappe, S.W., Cappaert, J.M., Trappe, T.A. (Eds.), Biomechanics and Medicine in Swimming, vol. VII. E & FN Spon, New York, pp. 53–58.

Dowling, A., Corazza, S., Chaudhari, A.M.W., Andriacchi, T.P., 2010. Shoe-surface friction influences movement strategies during a sidestep cutting task: implications for anterior cruciate ligament injury risk. American Journal of Sports Medicine 38 (3), 478–485.

Gourgoulis, V., Aggeloussis, N., Kasimatis, P., Vezos, N., Boli, A., Mavromatis, G., 2008. Reconstruction accuracy in underwater three-dimensional kinematic analysis. Journal of Science and Medicine in Sport 11, 90–95.

Heikkila, J., Silven, O., 1997. A four-step camera calibration procedure with implicit image correction. In: IEEE Computer Society Conference on Computer Vision and Pattern Recognition (CVPR'97), San Juan, Puerto Rico, pp. 1106–1112.

Holthe, M., McLean, S., 2001. Kinematic comparison of grab and track starts in swimming. In: Proceedings of the XIX International Society of Biomechanics in Sport Symposium, San Francisco, USA.

KadewTraKuPong, P., Bowden, R., 2001. An improved adaptive background mixture model for real-time tracking with shadow detection. In: Proceedings of the 2nd European Workshop on Advanced Video-based Surveillance Systems, Kingston upon Thames, UK.

Laurentini, A., 1994. The visual hull concept for silhouette base image understanding. IEEE Transactions on Pattern Analysis and Machine Intelligence 16, 150–162.

Lavest, J.M., Rives, G., Lapresté, J.T., 2003. Dry camera calibration for underwater applications. Machine Vision and Applications 13 (5–6), 245–253.

Maglischo, E.W., 2003. Swimming Fastest. Human Kinetics, Champaign.

Mündermann, L., Corazza, S., Andriacchi, T.P., 2007. Accurately measuring human movement using articulated ICP with soft-joint constraints and a repository of articulated models. In: IEEE Computer Society Conference on Computer Vision and Pattern Recognition (CVPR '07), Minneapolis, USA.

Mündermann, L., Corazza, S., Andriacchi, T.P., 2006. The evolution of methods for the capture of human movement leading to markerless motion capture for biomechanical applications. Journal of NeuroEngineering and Rehabilitation 3, 6.

Mündermann, L., Corazza, S., Chaudhari, A.M., Alexander, E.J., Andriacchi, T.P., 2005. Most favorable camera configuration for a shape-from-silhouette markerless motion capture system for biomechanical analysis. In: Proceedings of the SPIE-IS&T Electronic Imaging—2005, San Jose, USA.

Ohgi, Y., 2002. Microcomputer-based acceleration sensor device for sports biomechanics—stroke evaluation by using swimmer's wrist acceleration. In: Proceedings of the 1st IEEE international Conference on Sensors, Orlando, USA.

Sigal, L., Black, M., 2010. Guest Editorial: state of the art in image- and video-based human pose and motion estimation. International Journal of Computer Vision 87 (1–2), 1–3.

Schleihauf, R.E., Gray, L., DeRose, J., 1983. Three-dimensional analysis of swimming propulsion in the sprint front crawl stroke. In: Hollander, A.P., Huijing, P.A., de Groot, G. (Eds.), Biomechanics and Medicine in Swimming. Human Kinetics, Champaign, IL, pp. 173–184.

Slawson, S.E., Conway, P.P., Justham, L.M., West, A.A., 2010. The development of an inexpensive passive marker system for the analysis of starts and turns in swimming. Procedia Engineering 2 (2), 2727–2733.

Slawson, S.E., Justham, L.M., West, A.A., Conway, P.P., Caine, M.P., Harrison, R., 2008. Accelerometer profile recognition of swimming strokes. In: Estivalet, M., Brisson, P. (Eds.), The Engineering of Sport, 7. Springer-Verlag, Paris, pp. 81–87.